JOURNAL OF SOLID STATE CHEMISTRY 10, 312–322 (1974)

Multiple Phases in the System MgF_2–Nb_2O_5
An Electron Microscope Study of Intergrowths, Defects, and Disordered Crystals

J. L. HUTCHISON, F. J. LINCOLN,* AND J. S. ANDERSON

Inorganic Chemistry Laboratory, University of Oxford, England

Received September 10, 1973

Mixtures of $MgF_2 \cdot xNb_2O_5$ with $x = 7$ and 14 have, on annealing at high temperatures yielded a wide variety of block structures in which MgF_2 has replaced MeO_2 ($Me = Ti^{4+}, Nb^{4+}$). With F^- stabilizing the formation of large blocks, numerous defect structures have been characterized by direct lattice resolution electron microscopy. Features thus observed include planar faults, intergrowths, segregated domain structures, and disordered crystals. Chemical implications of these features are discussed.

1. Introduction

A detailed study of the MgF_2–Nb_2O_5 system, using electron diffraction and direct lattice imaging techniques, has revealed the existence of a number of phases within the composition range $MeX_{2.417}$–$MeX_{2.500}$, where $Me = Mg, Nb$; $X = 0, F$ (*1*). These mixed cation oxyfluorides have structures similar to those of the mixed-valence binary niobium oxides and the ternary titanium niobium oxides within the same composition range (*2*); the similarity in ionic radii (crystal radius of $Mg^{2+} = 0.66$, of $Ti^{4+} = 0.68$, of $Nb^{5+} = 0.69$ Å; of $O^{2-} = 1.32$ Å, of $F^- = 1.33$ Å) makes substitution on both cation and anion sites possible. An electron microscope study of the TiO_2–Nb_2O_5 system published by Allpress (*3*) revealed a number of new phases based on the intergrowth of simple block structures, and more recent work has shown that similar, though more restricted, intergrowth structures and defects occur in the binary oxide system (*4–6*). In the mixed cation oxyfluorides, the possibility of compensatory substitution of F^- for O^{2-}, in addition to replacement of Nb^{5+} by Mg^{2+}, means that each block structure, with a defined anion:cation ratio, corresponds to a range of isostructural solid solutions. The compound $MgNb_{14}O_{35}F_2$ described by Lundberg (*7*) is only one arbitrary composition within the structure type determined.

It is known that the presence of F^- ions stabilizes columns of larger cross section or length in block structures (*8*). This is understandable in terms of the net electrostatic charge distribution within these structures: preferential substitution of F^- for O^{2-} (or of W^{6+} for Nb^{5+}) in the interior coordination octahedra of the columns would minimize the local unbalance of ionic charge.

1.1. Block Structures

The basic principles of block structures have been adequately described elsewhere (*2*). They are built up from columns of apex-linked octahedra, finite in cross section and infinite along the *b*-axis of the structure. Blocks in adjacent columns at levels $y = 0$, $y = 1/2$ are linked by edge-sharing, while blocks at the same level are linked either by additional edge-sharing, or they may enclose tunnels in which the metal atoms are usually

* Chemistry Department, University of Western Australia, Nedlands, W.A.

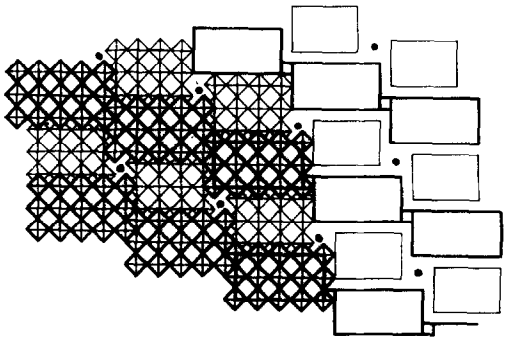

FIG. 1. [010] projection of H–Nb_2O_5 structure, with columns of [NbO_6] octahedra, (5 × 3) in cross section at one level (heavy lines) and (4 × 3) at alternate levels (light lines). The schematic representation is also shown. Positions of tetrahedrally coordinated cations shown as dots.

in tetrahedral configuration. An idealized projection of a typical block structure is shown in Fig. 1.

1.2. Disorder in Block Structures

Disorder is usually associated with intergrowth of blocks of different cross section or configuration from those of the perfect host lattice, and may or may not be accompanied by a change in composition. Conversely, local changes in composition usually involve intergrowths of different block geometry (*9*). Coherent intergrowth is in principle possible where structures have geometrically compatible interfaces and isolated, random lamellae of a different structure coherently intergrown with a host have been termed Wadsley defects. Another possible type of disorder is the coherent intergrowth of larger domains of different structures. Thirdly, there is the possibility of a high degree of disorder, with respect to the superstructure, in crystals which still maintain good order within and along the individual columns. Actual dislocations of the subcell, involving elastic distortion, are occasionally observed, but are beyond the scope of this present paper and will be discussed elsewhere.

The purpose of this paper is, therefore, to describe the defect structures observed in the various $MgF_2 \cdot xNb_2O_5$ phases, as determined by high resolution electron microscopy.

2. Experimental

2.1. Preparation of Materials

Johnson–Matthey "Spec-Pure" MgF_2 and Nb_2O_5 were mixed in molar proportions 1:7 and 1:14. The 1:7 mixture was heated in a sealed platinum tube for 160 hr at 1270°K (Sample 1); the 1:14 mixture was heated for 160 hr at 1510°K (Sample 2) and for a further 160 hr at 1670°K (Sample 3). After heating, the samples were cooled rapidly to room temperature. Samples were prepared for examination in a JEM 100U electron microscope by techniques already described (*10*). Crystals were supported in holey carbon films and suitably oriented, thin fragments overlying holes were photographed free of background noise, at a magnification of about ×250 000.

2.2. Interpretation of Lattice Images

Recent work (*10*, *11*) has shown that under certain conditions, high resolution lattice images of complex oxide structures may be interpreted as projections of the potential distribution within the crystal. Although the complete theory for these images had not yet been fully developed, the limitations apply mainly to the thickness of the crystal (~100 Å), the accuracy of orientation with respect to the electron beam (within 10^{-3} rad) and the amount of defocus of the electron microscope (*12*). In the micrographs presented here these factors were taken into account and in each case it was possible to derive the detailed structures of defects unambiguously, the densely populated sheets of atoms (shear planes) bounding the columns being clearly resolved as prominent, dark lines.

3. Results

The electron microscope study of the distribution of phases within the MgF_2–Nb_2O_5 system (*1*) revealed the existence of the structure types shown in Table I. As already stated, each of these structures can give rise, by compensatory substitution, to a solid solution range with the general composition set out in the last column.

These various structures have been identi-

TABLE I

OBSERVED STRUCTURES AND SOLID SOLUTION TYPES

$Me_{28}X_{70}$	$(4 \times 3)_1 + (5 \times 3)_\infty$ ($H\text{-}Nb_2O_5$ type)	$Mg_xNb_{28-x}O_{70-3x}F_{3x}$
$Me_{16}X_{40}$	$(4 \times 4)_\infty$ ($N\text{-}Nb_2O_5$ type)	$Mg_xNb_{16-x}O_{40-3x}F_{3x}$
$Me_{18}X_{45}$	$(6 \times 3)_\infty$	$Mg_xNb_{18-x}O_{45-3x}F_{3x}$
$Me_{25}X_{62}$	$(4 \times 3)_2$	$Mg_xNb_{25-x}O_{63-3x}F_{3x-1}$
$Me_{15}X_{37}$	$(5 \times 3)_\infty$	$Mg_xNb_{15-x}O_{38-3x}F_{3x-1}$
$Me_{12}X_{29}$	$(4 \times 3)_\infty$	$Mg_xNb_{12-x}O_{31-3x}F_{3x-2}$
$Me_{53}X_{132}$	1:1 intergrowth of $Me_{28}X_{70}$ and $Me_{25}X_{62}$	$Mg_xNb_{53-x}O_{133-3x}F_{3x-1}$
$Me_{39}X_{97}$	1:2 intergrowth of $Me_{28}X_{70}$ and $Me_{25}X_{62}$	$Me_xNb_{78-x}O_{196-3x}F_{3x-2}$
$Me_{103}X_{256}$	1:3 intergrowth of $Me_{28}X_{70}$ and $Me_{25}X_{62}$	$Mg_xNb_{103-x}O_{259-3x}F_{3x-3}$

fied and described elsewhere, but the intergrowths between separate phases and more complex defect structures have not been discussed. They may be classified into a number of distinct groups. It may be noted that a four component system, with phases of variable composition, is involved. In such a system, three solid phases of variable composition can coexist, with the chemical potentials fixed through the partial pressure of some volatile species (e.g., NbF_5 or $NbOF_3$), either as separate crystals or, subject to the topology of coherent intergrowth, as domains within a single crystal. The coexistence of phases or structures does, however, imply a spatial fluctuation in composition which, in the case of domain structures, must be perpetuated and propagated in the process of crystal growth.

3.1. Isolated Wadsley Defects

Figure 2 illustrates a typical, single Wadsley defect (arrowed) in a fragment of $Me_{25}X_{62}$ (Sample 3), in which outlines of blocks and the tetrahedral sites at the corners of pairs of blocks are clearly resolved in the lattice image. The structure of the host consists of columns of (4×3) octahedra, linked together in pairs by edge-sharing. As a descriptive aid, it is said to be composed of "*C*-rows" (3). The defect (arrowed) is a row consisting of alternate (4×3) and (5×3) blocks, and is of the structure-type $Me_{28}X_{70}$ of which $H\text{-}Nb_2O_5$ is the end member. ("*D*-rows").

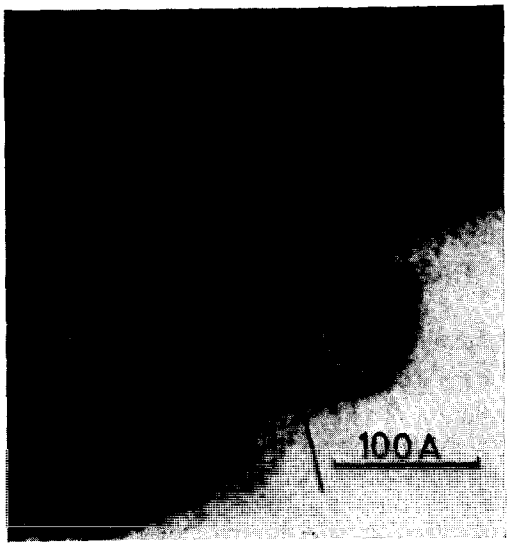

FIG. 2a. Lattice image of $Me_{25}X_{62}$ structure, containing a single Wadsley defect (arrowed), of $Me_{28}X_{70}$ structure.

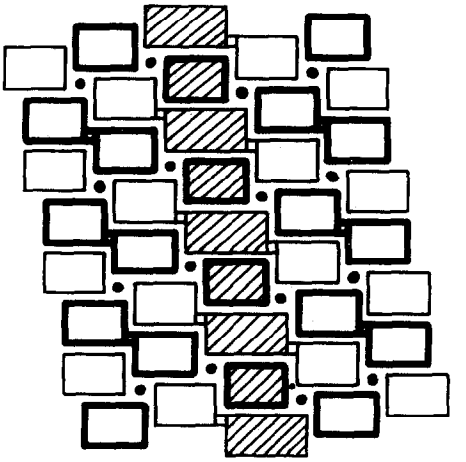

FIG. 2b. Idealized structure of the defect slab (shaded) and its surrounding host structure.

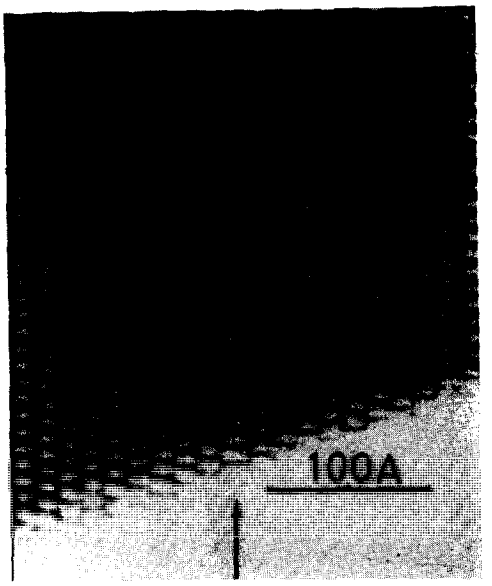

FIG. 3a. Lattice Image of $Me_{12}X_{29}$ structure, with a single Wadsley defect (arrowed) consisting of (5 × 3) blocks, $Me_{15}X_{37}$.

Occasionally Wadsley defects "jog" sideways, perpendicular to the *b*-axis (*13*). This is illustrated in Fig. 3a in which the host lattice consists of (4 × 3) columns corresponding to the structure $Me_{12}X_{29}$ (Sample 3). A single planar defect (arrowed) which consists of a row of (5 × 3) columns ($Me_{15}X_{37}$) alters its position within the crystal, by one row, in region 'A'. The dark contrast within this region is consistent with a series of three overlapping structures along the *b*-axis. It can be seen from the idealized diagrams of this region (Figs. 3b, c) that the lateral shift of this defect takes place *via* a stepped structure in the shear plane.

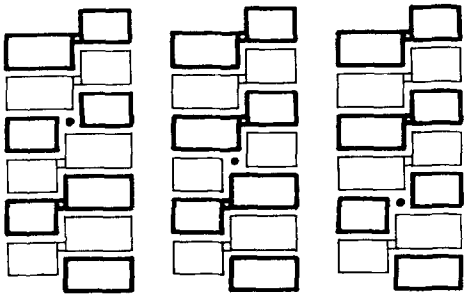

FIG. 3b. The three overlapping structures which account for the contrast in the area *A* in Fig. 3a.

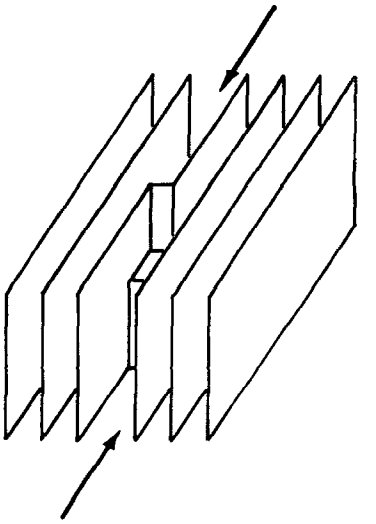

FIG. 3c. Diagrammatic representation of a "jog" perpendicular to *b*.

3.2. Intergrowths

3.2.1. Ordered Structures. When Wadsley defects are present in sufficient numbers, they may arrange themselves to form new

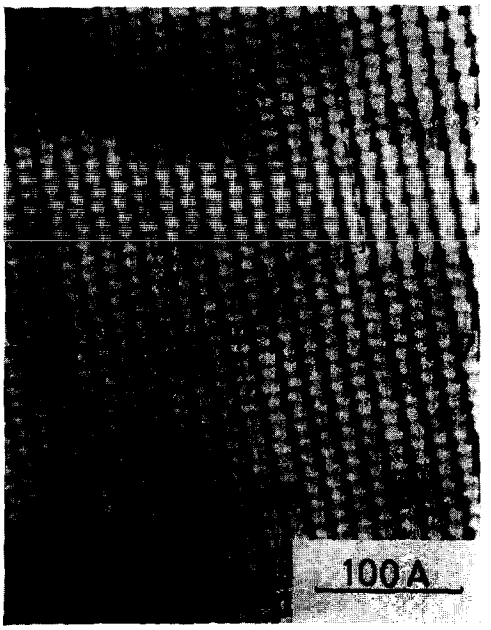

FIG. 4. Lattice Image of a crystal fragment containing lamellae of $Me_{25}X_{62}$ (*C*-rows) and $Me_{28}X_{70}$ (*D*-rows) The *D*-rows are numbered. The area enclosed by dashed lines is a domain of $Me_{39}X_{97}$.

FIG. 5a. Lattice Image of a fragment containing three different structures coherently integrown; $Me_{15}X_{37}$ (A), $Me_{28}X_{70}$ (B) and $Me_{12}X_{29}$ (C).

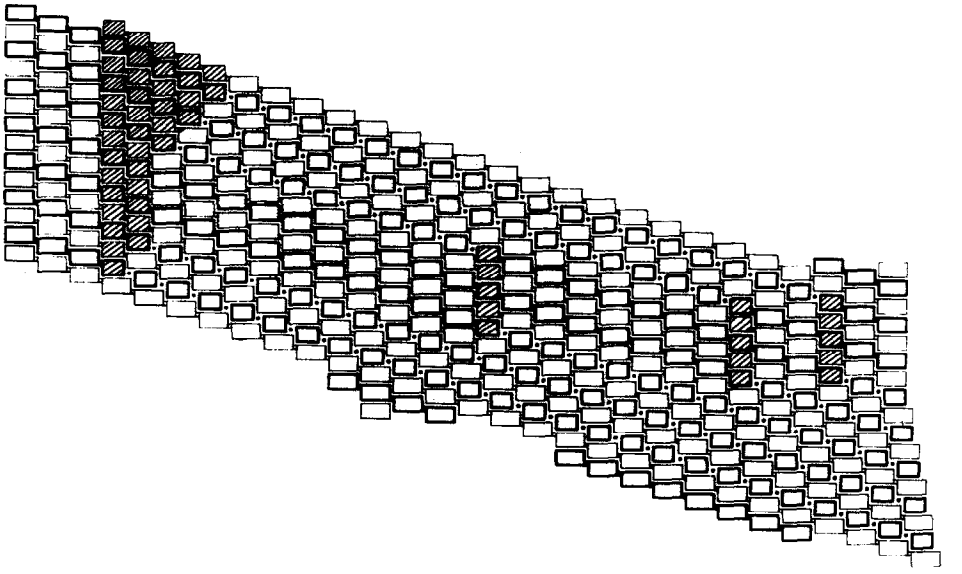

FIG. 5b. Idealized structure of part of (a) showing the distribution of structures. $Me_{12}X_{29}$ is shaded.

intergrowths with lamellae of the host lattice, giving structures which are intermediate in composition. Identification of defined intergrowths, as distinct from the effect of random interpolation, is dependent on the recurrence of certain stacking sequences. When only a small number of sequences corresponding to one structure is observed consecutively, then its definition as a new "phase" becomes questionable. These considerations are discussed more fully in a previous paper (*1*).

Thus Allpress (*3*) identified a series of intergrowths between $TiNb_{24}O_{62}$ (*C*-rows) and H–Nb_2O_5 (*D*-rows). In the MgF_2–Nb_2O_5 system, a similar, though more extensive, series of intergrowth structures was observed in the range $Me_{2.480}$–$Me_{2.500}$ as intergrowths between the $Me_{25}X_{62}$ and $Me_{28}X_{70}$ series.

The lattice image in Fig. 4 shows a crystal fragment (Sample 3) containing (over the total area observed) a mixture of 70% *C*-rows and 30% *D*-rows. In this crystal it was possible to identify domains of $Me_{39}X_{97}$, $Me_{53}X_{132}$ and $Me_{103}X_{256}$ (*1*). Since these domains are built up from ordered sequences of *C* and *D*-rows, it is obvious that the domains will be bounded on two sides by either a *C* or a *D* row. If such a row alters its position, then the domain wall will correspondingly wander through the crystal. In Fig. 4, *D* rows "3" and "6" enclose an ordered array ...*CCDCCDCC*..., which defines the structure $Me_{39}X_{97}$ in the upper half of the picture; in the lower half the domain of $Me_{39}X_{97}$ has been decreased in width from 140 Å down to 47 Å, equivalent to one unit-cell, as a result of a lateral repositioning of *D*-row 5 in the crystal. At the top of the micrograph, this row is inside the domain of $Me_{39}X_{97}$. After its slip sideways, the domain boundary is effectively altered, so as to exclude row 5 from the final, narrow lamella of $Me_{39}X_{97}$.

3.2.2. Segregation of Structures. The lattice image of a crystal fragment of Sample 2 is shown in Fig. 5a. In the area shown the material has segregated into three distinct, but interconnected and fully coherent structures; $Me_{15}X_{37}$, consisting of parallel rows of (5 × 3) blocks (domains "A"), "H–Nb_2O_5 structure," alternate strips of (5 × 3) blocks linked in

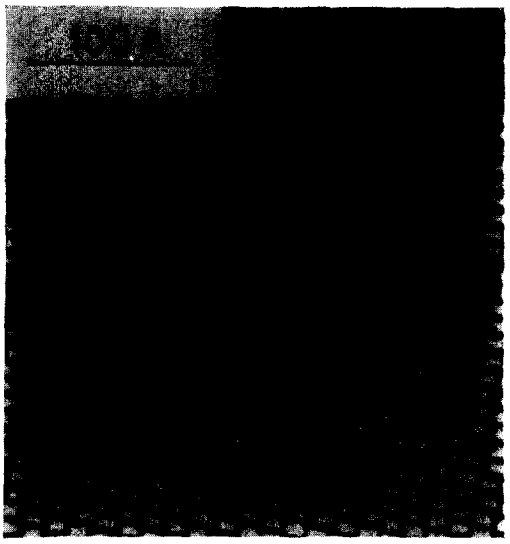

FIG. 6. Lattice Image, showing domains (E) of $Me_{25}X_{62}$ coherently intergrown with domains (*F*) of $Me_{12}X_{29}$.

ribbons and (4 × 3) blocks linked by tetrahedral sites (domains "*B*") and $Me_{12}X_{29}$—parallel rows of (4 × 3) blocks (domains "*C*").

In this example the three intergrowth structures involve different combinations of two block sizes, (4 × 3) and (5 × 3). These areas must differ in composition, but are related through the equilibrium condition already stated. An alternative is for the different intergrowths to be built up from blocks of one size, differing only in configuration. An example of this is shown in Fig. 6. In this crystal fragment (Sample 3) domains of $Me_{25}X_{62}$(*E*) consisting of (4 × 3) blocks in pairs are intergrown coherently with domains (*F*) of $Me_{10}X_{29}$, in which the (4 × 3) blocks are in ribbons. Thus composition changes across this particular crystal are accommodated by alterations in the block configuration, without altering their dimensions; it is interesting to note that ordered intergrowths between these two structures were not observed.

3.2.3. "*Island Intergrowth.*" Occasionally small, isolated domains of one structure may be completely surrounded, or trapped in the host, and appear as small fully coherent islands in the host structure. This is illustrated

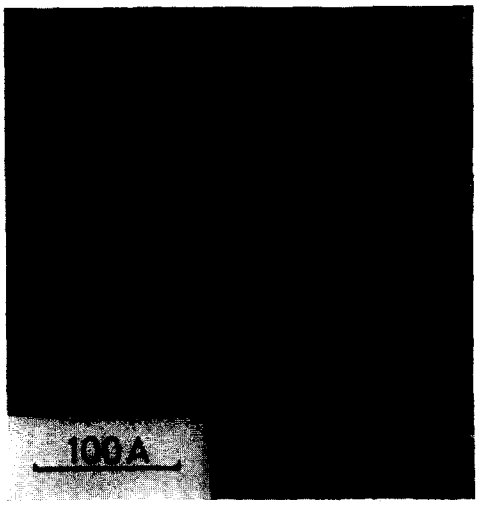

FIG. 7a. Lattice Image of $Me_{16}X_{40}$ (N–Nb_2O_5-type)—(4 × 4) blocks, containing a small domain (*I*) of $Me_{12}X_{29}$—(4 × 3) blocks.

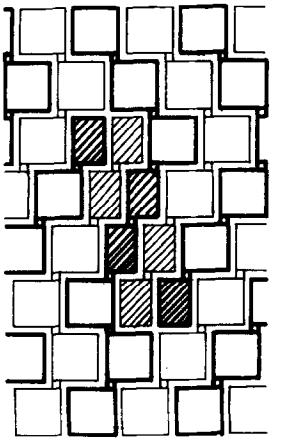

FIG. 7b. Idealized structure of domain *I* (shaded) and its surroundings.

in Fig. 7 (Sample 1), where there is a small domain (*I*) of $Me_{12}X_{29}$ in a domain of "N–Nb_2O_5" structure ($Me_{16}X_{40}$, with (4 × 4) blocks.) This domain, only eight columns in extent, is perfectly accommodated within the host by means of stoichiometric (001) twinning of the N–Nb_2O_5 structure. The twinned N–Nb_2O_5 structure, an orthorhombic modification, has not hitherto been reported, although the analogous (4 × 3) $Nb_{12}O_{29}$ structures in binary as well as ternary oxides have been found and identified in this form (*14, 15*). In extensive observations on the N–Nb_2O_5 structure, to be reported later, we have frequently observed both (001) twinning and more extensive lamellae of the orthorhombic form. The small island thus bounded defines a region of the crystal rich in MgF_2 and is probably the result of highly localized impurity segregation.

3.2.4. Partly coherent domain boundaries. Because of the strict geometrical limitations governing intergrowth between different structures, there are numerous "forbidden" intergrowths. Such mutually incompatible structures will attempt to intergrow only where the growth fronts of separate crystals or domains, or of dendrites related through origin in a common nucleus, happen to impinge. Intergrowth may be induced by a sufficient (but still, apparently, very subtle) fluctuation in the local environment of a growing crystal. Observations suggest that a new structure and composition of growth may then be initiated along one segment only of a permitted, coherent growth plane; as the original and new domains are propagated, the interface between them may have no possibility of conforming to coherent geometry. The hybrid crystal which then forms is required to fill the resultant mismatch region between two perfect structures. If local order and the "block principle" govern the structures formed, this may well involve blocks of peculiar shape and size which necessitate an overall composition in this region which may be quite different from that of either component structure. Figure 8 shows a crystal (Sample 3) containing domains "*J*" and "*K*" of $Me_{25}X_{62}$, $(4 \times 3)_2$ and $Me_{12}X_{29}$, $(4 \times 3)_\infty$. In section 3.2.2 (Fig. 6) it was shown that coherent intergrowth was possible between these two structures, $(001)_{Me_{25}X_{62}}$ and $(20\bar{1})_{Me_{12}X_{29}}$ being compatible planes. This interface is again seen in Fig. 8, along the line *XY*. The interface *XZ*, however, does not correspond to a coherent interface, and it necessarily contains blocks of anomalous sizes and configurations. The region of intergrowth (outlined) is seen to contain (3 × 3), (3 × 4), (3 × 5) and (3 × 6) blocks

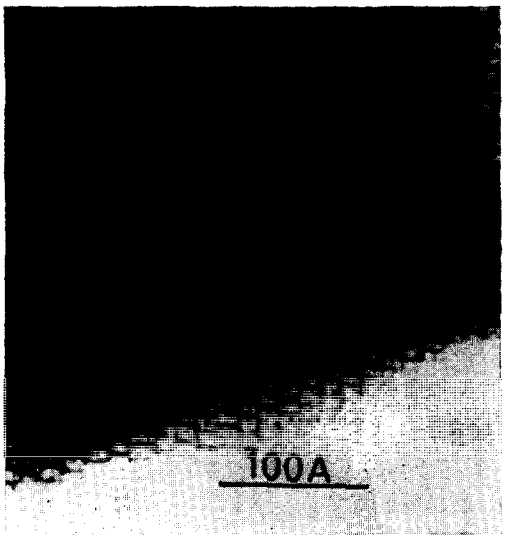

FIG. 8a. Lattice Image of boundaries between $Me_{25}X_{62}$ (J) and $Me_{12}X_{29}$ (K). The boundary XY is completely coherent, whilst XZ is only partly coherent, containing anomalous blocks.

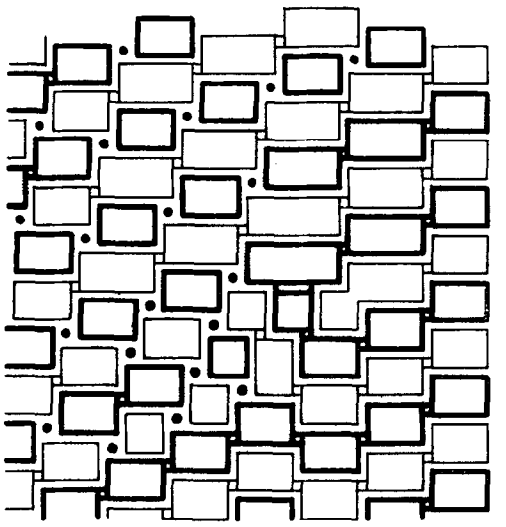

FIG. 8b. Idealized structure of part of the region within the boundary XZ.

(Fig. 8b). There is also a "T-block" in which (6 × 3) and (3 × 3) blocks on the same level are fused together by addition edge-sharing in the *ac* plane. Also, a (5 × 3) and (3 × 3) block on the same level are linked in such a way as to enclose a "rectangular tunnel" (*16*).

Domain boundaries may become progressively less coherent—from the stage where they include a varied mixture of blocks, through the stage where the "block principle" is partly disobeyed—the "filler" structure is not completely space filling. This is evident in the "rectangular tunnels" described in (*16*) and in other mismatch regions. Finally, boundaries may become incoherent and in a few cases there is evidence for actual dislocations, containing edge and screw components, in the sublattice. These will be described elsewhere.

3.3. *Defects Perpendicular to the* b-*Axis*

In Fig. 3 a single Wadsley defect was shown to alter its position in the lattice by means of a step, where blocks of one size were overlain by those of another. In Fig. 9 (Sample 3) the lattice image shows a crystal consisting mainly of $Me_{25}X_{62}$ (C-rows) with several D-rows (numbered) intergrown randomly. The two adjacent D-rows labelled "4" and "5" are seen to traverse the lattice across a region containing a high concentration of the dark contrast corresponding to tetrahedral sites. The contrast in this region suggests that the sideways displacement of D-rows 4 and 5 takes place via a sequence of "steps" in the lattice. These "steps" which displace the D-rows in a direction perpendicular to the *b*-axis are shown schematically in Fig. 8b and c. Iijima (*6*) has pointed out that, for relatively simple "one-step" displacements there are two possible arrangements: either a single, nonrecurrent step, or a series of alternating layers of the two structures. He suggested that the single-step structure was more likely. A similar argument may be applied to the more complex multistep displacement shown here; and again it seems likely that the actual structure within the crystal is more accurately depicted as a nonrecurrent series of single steps, rather than a zigzag arrangement of recurrent "jogs".

3.4. *Localized Disorder*

Subtle variations in either component concentrations or impurity levels, or in local

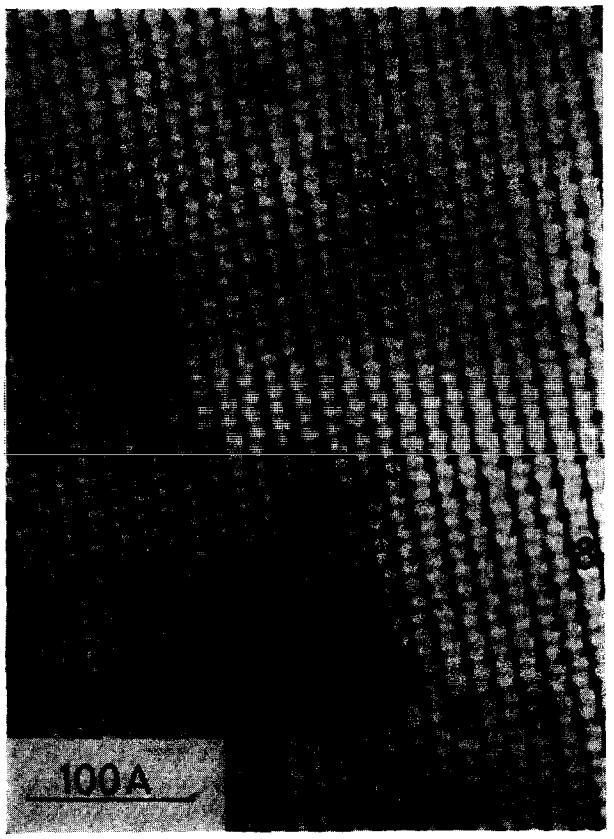

FIG. 9a. Crystal fragment containing $Me_{25}X_{62}$ (*C*-rows) and lamellae of $Me_{28}X_{70}$ (*D*-rows, numbered 1–8) *D*-rows 4 and 5 move laterally via an area of dense contrast.

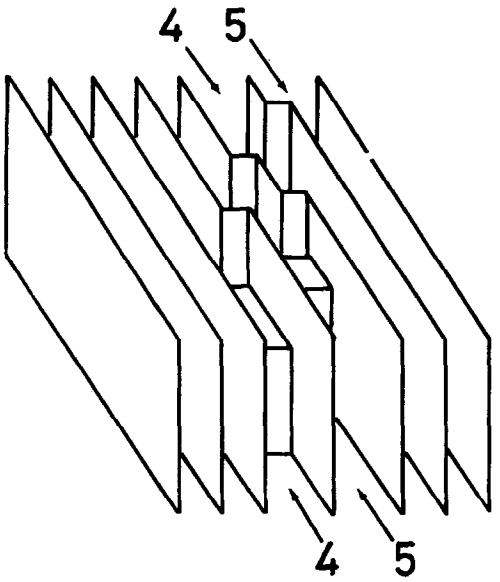

FIG. 9b. Schematic representation of the series of "jogs" in 9a.

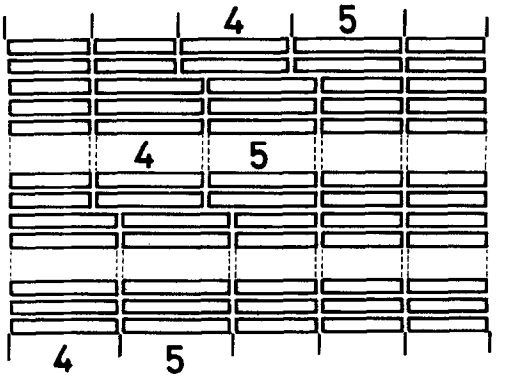

FIG. 9c. Schematic view along the direction of the arrows in 9b showing overlapping *C* and *D* rows.

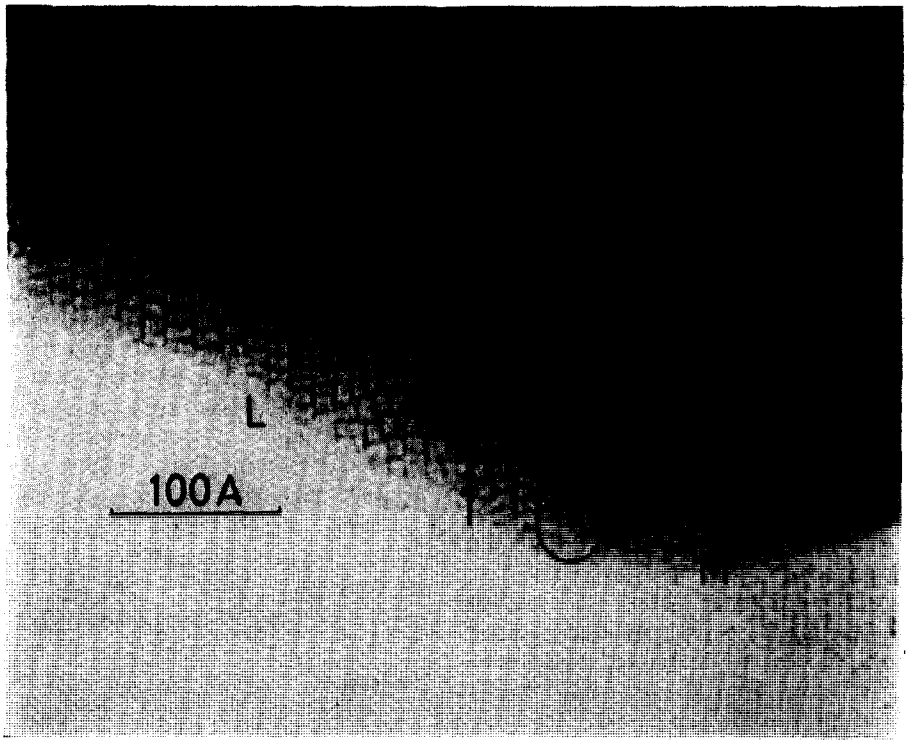

FIG. 10a. Lattice Image of $Me_{12}X_{29}$ structure containing an extensive region of severally disordered block structure. An anomalous block is enclosed by a circle.

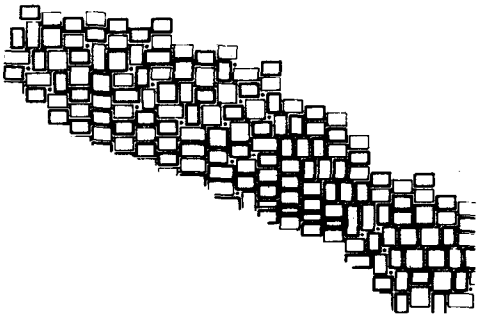

FIG. 10b. Idealized structure of area *L*.

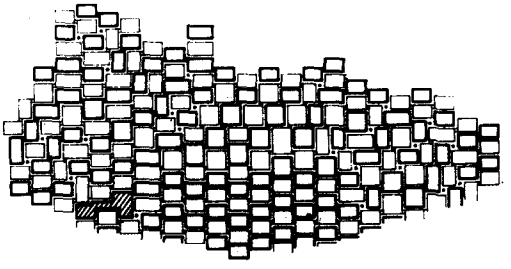

FIG. 10c. Idealized structure of area *M*. The anomalous block is shaded.

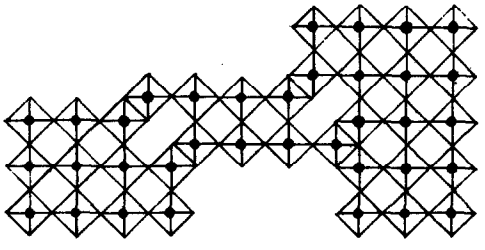

FIG. 10d. Details of the anomalous block enclosed in circle.

temperature conditions, may occasionally give rise to regions or extreme disorder. In Fig. 10a the lattice image shows evidence of well-ordered $Me_{12}X_{29}$ structure extending into the thicker regions of the crystal, and also at the thin fracture edge. There is no evidence for disorder having been generated during the grinding of the sample, as the edge appears to cut through individual blocks. There is (stoichiometric) (001) twinning, and occasional single rows of (5 × 3) blocks are the

TABLE II

Block size	Compositions	Structure type
4 × 2	2.250	Me_8X_{18}[a]
4 × 3	2.417	$Me_{12}X_{29}$
5 × 3	2.467	$Me_{15}X_{37}$
6 × 3	2.500	$Me_{18}X_{45}$
4 × 4	2.500	$Me_{16}X_{40}$
5 × 4	2.550	$Me_{20}X_{51}$
$(4 \times 3)_1$	2.538	$Me_{13}X_{33}$

[a] (4 × 2) blocks have not been previously observed in niobium oxide structures.

only lattice variations in these parts of the crystal. There is, however, an extensive region of extremely disordered structure, in which the "crystal" is built up from a wide variety of small domains of perfect structure and of individual blocks of different sizes. The range of observed block dimensions, and their corresponding compositions and "structure types" are listed in Table II.

The occurrence of this wide range of structures within an extensive domain of an otherwise nearly perfect crystal raises a number of problems about the mechanism of crystal growth. Because each structure type can accommodate variations in the ratio of the components, within a solid solution range, or by coherent growth of another, coexisting structure, as permitted by the phase rule, it would appear from the evidence that fluctuations in growth conditions normally result in well ordered domain structures. In the present instance, the block structure principle of short range order is preserved, but the multiplicity and arrangement of blocks with different, and in some cases abnormal, sizes and compositions suggest that order and spatial uniformity of composition has been lost; the growing crystal has simply filled space, in the manner of a jigsaw puzzle. Moreover, this has been done not merely in building up a single layer, but in three dimensions. In all these crystals, the *b*-axis of the crystal is the direction of rapid growth; successive layers must be laid down more rapidly than the rate at which the array of columns grows outwards in the *a*–*c* plane. Successful lattice imaging implies that the crystal is highly ordered along the direction of the electron beam, and the section observed, probably 50–150 Å—i.e., up to 40 or so layers —thick is presumably representative of a significant slice of the original crystal. It would follow that the singularity in structure and composition has been replicated as each successive (010) plane has been built up.

This problem—the propagation of Wadsley defects, domain walls, fluctuations in composition and structure, etc.—recurs continually in the electron microscopy of defect structures, and there is a need to investigate the mechanism by which crystals of complex structure grow, both by solid state reactions and by vapour transport processes.

References

1. F. J. LINCOLN, J. L. HUTCHISON, AND J. S. ANDERSON, *J. Chem. Soc.* (*Dalton Trans.*) 115 (1974).
2. R. GRUEHN, N.B.S. Special Publication 364, Solid State Chemistry, p. 63 (1972).
3. J. G. ALLPRESS, *J. Solid State Chem.* **1**, 66 (1969).
4. J. S. ANDERSON, J. M. BROWNE, AND J. L. HUTCHISON, *J. Solid State Chem.* **5**, 419 (1972).
5. J. S. ANDERSON AND K. M. NIMMO, *J. Chem. Soc.* (*Dalton Trans.*) 2328 (1972).
6. S. IIJIMA, *Acta Cryst.* **A29**, 18 (1973).
7. M. LUNDBERG, *J. Solid State Chem.* **1**, 463 (1970).
8. A. D. WADSLEY AND S. ANDERSSON, "Perspectives in Structural Chemistry" (J. D. Dunitz and J. A. Ibers) Wiley, New York, 1970, **3**, 1.
9. J. S. ANDERSON, J. M. BROWNE, AND J. L. HUTCHISON, *Nature* (*London*) **237**, 151 (1972).
10. J. L. HUTCHISON AND J. S. ANDERSON, *Phys. Status Solidi* (a) **9**, 207 (1972).
11. S. IIJIMA, *J. Appl. Phys.* **42**, 5891 (1971).
12. J. M. COWLEY AND S. IIJIMA, *Z. für Naturf.* **27a**, (1972).
13. J. G. ALLPRESS, *J. Solid State Chem.* **2**, 78 (1970).
14. A. D. WADSLEY, *Acta Cryst.* **14**, 664 (1961).
15. R. NORIN, *Acta Chem. Scand.* **17**, 1391 (1963); **20**, 871 (1966).
16. J. L. HUTCHISON AND F. J. LINCOLN, *Phys. Status Solidi* (a) **17**, 169 (1973).